Available online at www.sciencedirect.com
ScienceDirect
Catalysis Today 137 (2008) 278–282
CATALYSIS TODAY
www.elsevier.com/locate/cattod

Adsorption of NO and NO_2 on ceria–zirconia of composition $Ce_{0.69}Zr_{0.31}O_2$: A DRIFTS study

B. Azambre [a,*], L. Zenboury [a], F. Delacroix [b], J.V. Weber [a]

[a] *Laboratoire de Chimie et Méthodologies pour l'Environnement (LCME), Université Paul Verlaine - Metz, Rue Victor Demange, 57500 Saint Avold, France*
[b] *ADEME, 2 Square La Fayette, 49004 Angers, France*

Abstract

In this study, the nature of surface intermediates generated by adsorption of NO and NO_2 on a commercial ceria–zirconia powder of composition $Ce_{0.69}Zr_{0.31}O_2$ was investigated using Diffuse Reflectance Infrared Fourier Transform Spectroscopy (DRIFTS). The conditions of occurrence of the main adsorbed species, i.e. nitrites and nitrates, are studied semi-quantitatively as a function of catalyst pre-treatment and/or type of adsorbed NO_x molecule. On the partially reduced ceria–zirconia, the primary role of NO_x is to re-oxidize the surface via adsorption/decomposition on reduced sites. By contrast, the formation of nitrites and nitrates readily occurs on oxidized surfaces, the latter kind of species being strongly promoted in the case of NO_2 adsorption only.

Keywords: Ceria–zirconia; $Ce_xZr_{1-x}O_2$; Adsorption; NO_x; DRIFTS; Nitrates

1. Introduction

The use of ceria in environmental catalysis has attracted much attention these recent years, namely as a key component in three-way-catalysts (TWC) or in soot abatement from diesel engine exhaust [1–4]. Apart from the treatment of emissions from mobile sources, applications of ceria-based materials include the removal of organics from wastewaters, and their use as additives in combustion processes or Fluid Catalytic Cracking (FCC) [1]. The strong redox properties of ceria are related to the facile oxidation/reduction of the cerium component with the concomitant creation/filling of oxygen vacancies. Among all ceria-related materials, ceria–zirconia $Ce_xZr_{1-x}O_2$ mixed oxides have known a particular interest due to their good thermal resistance to sintering and superior high Oxygen Storage Capacity (OSC) [1]. Within the $Ce_xZr_{1-x}O_2$ series, the redox properties of solid solutions strongly depend on their crystalline structures, the Ce/Zr ratio, the specific surface area and the presence of a promoter and accordingly, many nanostructural characterization studies have been made [1,5–8]. Noteworthy, it has been shown that the surfaces of some $Ce_xZr_{1-x}O_2$ monocrystals still include Ce^{3+} species and O vacancies after extensive oxidation in oxygen gas [9].

Despite the extensive literature existing both on the above-mentioned applications and nanostructural characterizations, there are only a few studies reporting the performances of ceria–zirconia as a support or catalyst in the Selective Catalytic Reduction (SCR) of NO_x by hydrocarbons, and most of these studies were using propene as reductant [10,11]. For NO_x-SCR, it is now clear that the mechanism involves a surface reaction between *ad*-N_xO_y and *ad*-HC intermediates, whose probability to occur at a given temperature depends on the intrinsic reactivity of the catalytic system and the relative surface coverages of the two adsorbates as well as their local structures. From a general viewpoint, the knowledge of the possible structures of surface *ad*-NO_x species and their routes of formation on metal oxides has been complicated by the fact that both surface acid–base and redox properties play a role in NO_x adsorption at the molecular level [12].

In this study, we aimed to investigate the adsorption/desorption behaviour of NO and NO_2 on a commercial ceria–zirconia ($Ce_{0.69}Zr_{0.31}O_2$) pre-treated under different conditions. A peculiar attention was paid to the nature of *ad*-NO_x species and the sites involved in their adsorption.

---

* Corresponding author. Tel.: +33 387939106; fax: +33 387939101.
E-mail address: bazambre@univ-metz.fr (B. Azambre).

0920-5861/$ – see front matter © 2007 Elsevier B.V. All rights reserved.
doi:10.1016/j.cattod.2007.09.003

2. Experimental

The $Ce_{0.69}Zr_{0.31}O_2$ sample used in this study was supplied by Rhodia France (La Rochelle) and obtained from nitrate precursors. XRD data (cubic lattice, space group $Fm3m$, $a = 0.530$ nm) and textural properties ($S_{BET} = 131$ m^2/g, pore volume = 0.3146 cm^3/g, average pore size = 10.2 nm) relevant to the characterization of this sample are described in more details elsewhere [11].

The structural characterization of the calcined ceria–zirconia by Raman spectroscopy was performed onto a Jobin-Yvon FT-Raman spectrometer (100 scans, resolution 2 cm^{-1}) with a double monochromator Spex and the 632.8 nm line of a He–Ne laser ($P = 9$ mW).

In situ diffuse reflectance infrared (DRIFTS) spectra generated upon exposure of the ceria–zirconia surface to NO or NO_2 at 30 °C were recorded onto pure samples using an environmental cell (Spectra-Tech) and a DRIFTS optical accessory (Graseby-Specac) attached to a Bio-Rad FTS 185 spectrometer. In order to investigate the effect of various pre-treatments on adsorption, the $Ce_{0.69}Zr_{0.31}O_2$ was pre-treated *in situ* inside the DRIFTS cell at 500 °C under synthetic air or Ar before admission of the reactive gas. Time-course difference spectra were calculated by taking as reference the Single-Beam (SB) spectrum of the ceria–zirconia just prior to NO or NO_2 adsorption.

3. Results and discussion

3.1. Structural properties of $Ce_{0.69}Zr_{0.31}O_2$

For comparison purposes, the FT-Raman spectrum of $Ce_{0.69}Zr_{0.31}O_2$ (calcined at 500 °C) is displayed together with that of ceria (CeO_2) in Fig. 1. As expected from the literature for a pure cubic fluorite structure [1,7], a single peak at 465 cm^{-1} (fundamental with F_{2g} symmetry) is observed for the CeO_2 reference (Fig. 1(a)). By contrast, the F_{2g} peak for $Ce_{0.69}Zr_{0.31}O_2$ is considerably lowered in intensity and broadens towards higher frequencies (new maximum at 477 cm^{-1} in Fig. 1(b)). These changes have to be connected with the increase of disorder in the fluorite structure and cell contraction upon partial substitution of Ce by Zr and/or existence of oxygen vacancies [1,7]. The appearance of weak bands *ca.* 304 and 625 cm^{-1} (Fig. 1(b)) is assigned to a tetragonal displacement of oxygen atoms from their ideal fluorite lattice positions [1]. According to the ceria–zirconia phase diagram and XRD results [1,11], these data seem consistent with the co-existence of small domains of cubic (c) and metastable tetragonal (t″) phases on $Ce_{0.69}Zr_{0.31}O_2$.

3.2. In situ DRIFTS of NO_2 adsorption at 30 °C on $Ce_{0.69}Zr_{0.31}O_2$

Time-course DRIFT difference spectra recorded during the exposure of $Ce_{0.69}Zr_{0.31}O_2$ to NO_2 (1000 ppm/Ar) at 30 °C are given for the 1800–700 cm^{-1} region in Fig. 2. These data were obtained using the spectrum of the pre-treated sample under air at 500 °C and cooled under Ar to 30 °C just before introduction of NO_2. Interpretation of these spectral data is based on common IR assignments of NO_x *ad*-species on metal oxides [13] and the known reactivity of ceria-based materials towards NO_x [9,14–16].

Up to 15–20 min of adsorption, difference spectra are dominated by a band *ca.* 1187 cm^{-1} attributed to the ν(N–O) vibrations of NO_2^- nitrites (Fig. 2) [13,16]. The low intensities

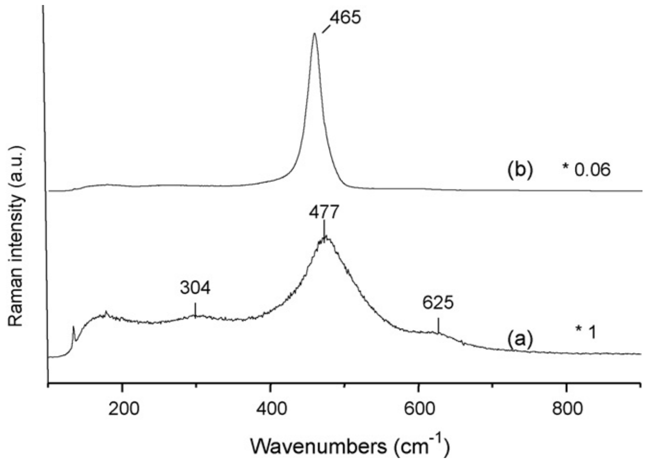

Fig. 1. FT-Raman spectra of (a) CeO_2 with cubic fluorite structure; (b) $Ce_{0.69}Zr_{0.31}O_2$.

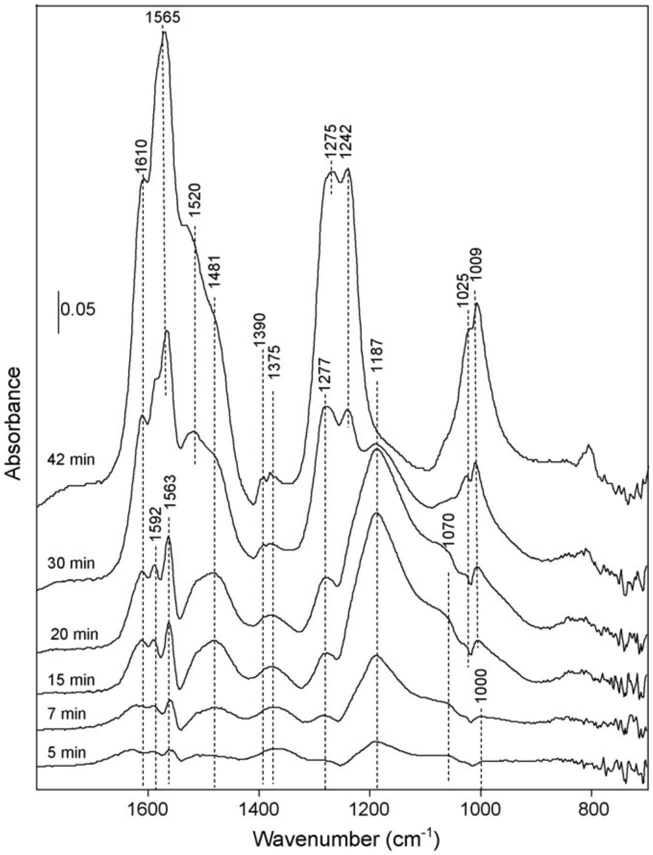

Fig. 2. Difference DRIFTS spectra in the 1800–700 cm^{-1} region corresponding to the adsorption of NO_2 at 30 °C on $Ce_{0.69}Zr_{0.31}O_2$ (pre-treated under air at 500 °C) after: 5, 7, 15, 20, 30, and 42 min.

observed in the 1520–1375 cm^{-1} region compared with those of the 1187 cm^{-1} band, indicate that these surface nitrites have in most case no corresponding $\nu(N{=}O)$ modes [13]. Hence, these surface nitrites are thought to preferentially adopt the bridged bidentate ($M_2(O_2){=}N^-$) and/or chelating bidentate ($M(O_2){=}N^-$) configurations. It has been shown recently that the (1 1 1) surface of $Ce_{0.8}Zr_{0.2}O_2$, even submitted to prolonged treatment in O_2, still contain some reduced Ce sites due to the increased stability of oxygen vacancy defects in comparison to those existing on ceria [9]. Here, the detection of surface nitrites on the air-pretreated $Ce_{0.69}Zr_{0.31}O_2$ surface is a clue for the presence of reduced sites. Bidentate nitrite species may have been formed by electron transfer from a reduced Lewis centre (Ce^{3+} or Zr^{x+}) to a NO_2 molecule with simultaneous re-oxidation of an oxygen vacancy, which can be depicted for instance as:

$$Ce^{3+}\text{-}\square\text{-}M^{x+} + NO_2 \rightarrow Ce^{4+}(ONO)^{-}M^{x+} \qquad (1)$$

Additionally, the bands *ca.* 1350, 1070 and 850 cm^{-1} are ascribed to the N–N (for the former) and N–O stretching modes (for the two latter), respectively, of *cis*-hyponitrites $N_2O_2^{2-}$ species (Fig. 2) [13,16]. Accounting for the existence of reduced sites on the air-pretreated $Ce_{0.69}Zr_{0.31}O_2$ surface, these species could have been formed in two steps involving: (i) the dissociation of NO_2 with simultaneous surface re-oxidation of vacancy defects; (ii) the subsequent adsorption of NO pairs (generated during (i)) via electron transfer from Ce^{3+} cations to yield $N_2O_2^{2-}$. According to [16], hyponitrites on ceria are not very thermally stable species and should decompose to N_2O. In our case, the existence of some adsorbed N_2O is revealed by the presence of a weak band at 2240 cm^{-1} [13]. During the same time period, other minor bands arising in the 1500–1300 cm^{-1} range are assigned to some monodentate nitrites, nitro or nitro-nitrito compounds (Fig. 2) [13]. On the other hand, a negative absorption develops *ca.* 3690 cm^{-1} (shoulders at 3740 and 3660 cm^{-1}) and weak positive absorptions are observed instead *ca.* 3630 and 3565 cm^{-1} (not shown here). These changes are due to the interaction and/or replacement of some ceria–zirconia hydroxyls with/by a NO_2 molecule. In the literature, similar red shifts in the positions of OH groups have been assigned either to an increased Brönsted acidity due to the withdrawing effect of the NO_2 moiety or as a result of hydrogen bond formation between slightly acidic OH and a NO_x molecule [13].

After 20 min of adsorption, the intensity of the 1187 cm^{-1} nitrite band decreases progressively at the expense of very strong bands, whose new maxima after 42 min on stream are 1009–1025, 1242–1275, 1520–1565–1585 and 1612 cm^{-1} (Fig. 2). As nitrites have no modes around 1000 cm^{-1}, this set of bands can be unambiguously ascribed to various kinds of surface nitrates [13]. According to Hadjiivanov and Vayssilov [13], the modes of bonding of NO_3^- species to the ceria–zirconia surface can be further distinguished by the extent of splitting between their $\nu_{as}(NO_2)$ and $\nu_s(NO_2)$ modes and the positions of the $(\nu_1 + \nu_3)$ combination modes in the 2650–2450 cm^{-1} region (not shown here). Here, the intense bands observed in our spectra *ca.* 1585–1565, 1275 and *ca.* 1010–1005 cm^{-1} (combination mode *ca.* 2565 cm^{-1}) can be ascribed to various kinds of chelating bidentate species whereas bridged bidentate nitrates are observed at 1610, 1220–1200 and 1010 cm^{-1} (combination band *ca.* 2610 cm^{-1}). Additionally, bands around 1530–1515, 1240 and 1030–1000 cm^{-1} (combination band *ca.* 2530 cm^{-1}) seem in good agreement with the existence of monodentate NO_3^- species (Fig. 2) [13].

Considering the decrease in the concentration of surface NO_2^- species after 20 min on stream, the formation of some of these NO_3^- species may involve, at least partially, the surface reaction of a nitrite species with an oxygen atom already present on the air-pretreated surface or left by the decomposition of a NO_2 molecule on a neighboured site:

$$NO_2^- + O(ads) \rightarrow NO_3^- \qquad (2)$$

In addition to this ‘‘nitrite route’’, the simultaneous growth of the nitrate bands with absorptions *ca.* 2300–2200, 2010 and 1934 cm^{-1} ascribed to NO_2^+ and/or NO^+ species (not shown here) indicates that other mechanisms could be operative. In that respect, the disproportionation of NO_2 in its dimerized form, i.e. N_2O_4, to give NO^+ and NO_3^- adsorbates that pair on acid–base sites has been proven by theoretical calculations to be a valid mechanism for a defect-free MgO surface and has been observed experimentally for other kinds of metal oxides [12]. Here, the disproportionation of NO_2 dimers is thought to contribute to the production of nitrates on defect-free crystal planes (the so-called ‘‘terrace’’ sites) of the ceria–zirconia.

3.3. DRIFTS study of NO adsorption at 30 °C—effect of pre-treatment conditions

When the DRIFTS study was repeated on the air-pretreated $Ce_{0.69}Zr_{0.31}O_2$ surface with NO instead of NO_2, rather similar spectra were obtained. For this reason, the corresponding spectra are not shown here. However, some changes were sometimes observed in the relative concentrations of the peculiar *ad*-NO_x species at a given adsorption time. In order to examine the respective effects of the nature of the reactive gas (NO or NO_2) and catalysts pre-treatments (500 °C under air or Ar) on the relative concentrations of the main adsorbed NO_x species, a semi-quantitative study was attempted using DRIFTS. Owing to absorptions in distinct spectral domains, peak fitting was not necessary and the intensities of the 1187 cm^{-1} (nitrites) and 1560 cm^{-1} bands (chosen as representative of nitrates) were measured directly from absorbance DRIFTS spectra. They are plotted in Fig. 3(A and B), respectively.

By comparing the signals obtained during the initial stages of adsorption (up to 20 min), it can be seen that the amount of nitrites and nitrates generated by NO and NO_2 on the air-pretreated $Ce_{0.69}Zr_{0.31}O_2$ catalyst is almost similar (Fig. 3(A)). This is explained by the strong oxidizing properties of some ceria–zirconia surface oxygens that promote the following reaction:

$$NO + (O)_{ads} = NO_2 \qquad (3)$$

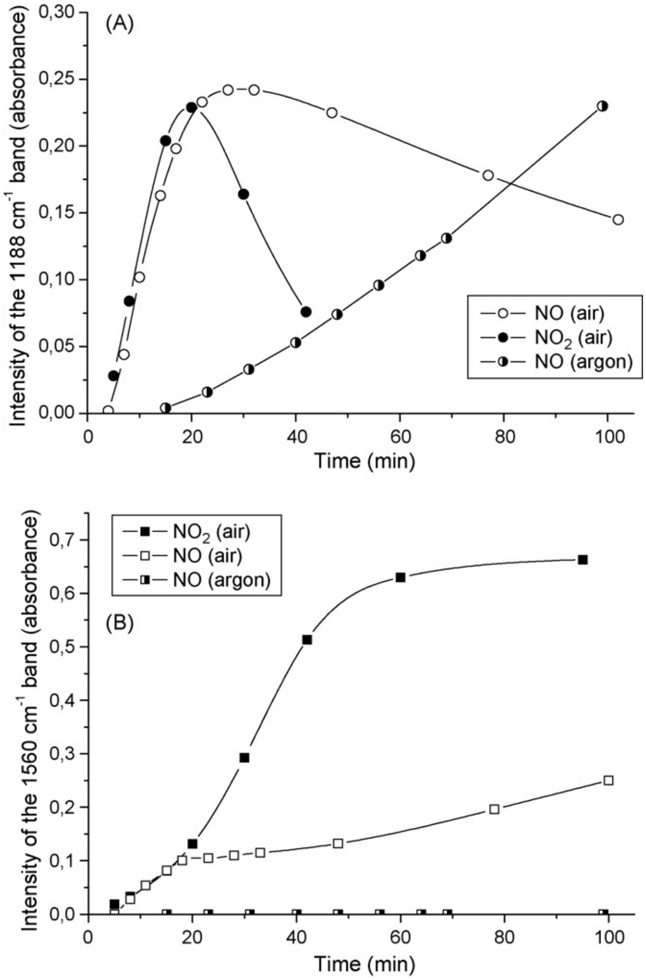

Fig. 3. Effect of pre-treatment conditions on the development with time of (A) the 1188 cm^{-1} (nitrites NO_2^-) and (B) the 1560 cm^{-1} (representative for nitrates NO_3^-) bands.

After 20 min adsorption, the decrease observed in the amount of surface nitrites is accompanied in both cases by the increase of nitrates (Fig. 3(B)). However, it is worth noting that the formation of nitrates from nitrites is strongly promoted for NO_2 adsorption but not for NO. This is in good agreement with the known relative oxidizing character of these two nitrogen oxides. Whereas NO_2 is a strong oxidizing agent, the effect of NO could be either reducing or oxidizing depending on the nature of the site.

Noteworthy, the argon-pretreated $Ce_{0.69}Zr_{0.31}O_2$ catalyst exhibits a marked different adsorption behaviour. First, nitrates were never observed even after more than 100 min exposure to NO (Fig. 3(B)). Second, the development of the nitrite band (now at 1194 cm^{-1}) is considerably delayed in comparison with the air-pretreated surface (Fig. 3(A)). By contrast, the characteristic absorptions of hyponitrites (1327 and 1063 cm^{-1}) and other easily removable *ad*-NO_x species (bands at 1640 and 1545 cm^{-1} tentatively assigned to N_2O^-) and a band at 2240 cm^{-1} (adsorbed N_2O) were observed during the first stages of adsorption (spectra not shown here). These discrepancies obviously reflect the differences existing in the amount of oxygen vacancy defects on the air- and argon-pretreated $Ce_{0.69}Zr_{0.31}O_2$ surfaces prior to adsorption. The pre-treatment of the $Ce_{0.69}Zr_{0.31}O_2$ catalyst under Ar is thought to create thermally induced oxygen vacancies and other kinds of defective sites more easily than the same pre-treatment performed under air. Therefore, reaction (3), which is needed for the formation of nitrites from NO, is hindered for the argon-pretreated surface in the first stages of NO adsorption. The primary role of NO is to re-oxidize the surface while undergoing decomposition or electron transfer reactions, such as leading to the formation of adsorbed $N_2O_2^{2-}$, N_2O and elemental N, O species. Whereas N and O *ad*-atoms are not detectable by FTIR, they were identified using XPS in other studies [12].

4. Conclusions

Using DRIFTS, the structures of *ad*-NO_x species generated by NO or NO_2 adsorption on ceria–zirconia $Ce_{0.69}Zr_{0.31}O_2$ surface characterized by different degrees of reduction were investigated. Whereas the quantity of oxygen vacancy defects and reduced metal centres was found to be not negligible for the air-pretreated surface, it was considerably more important for the argon-pretreated surface due to thermal reduction. As a consequence, the air-pretreated catalyst was able to readily promote the oxidation of NO to NO_2 at room temperature and the formation of bidentate nitrites, mainly via electron transfer. Upon increasing exposure to NO_x, nitrites transform via oxygen transfer to bidentate and monodentate nitrates, the latter process being especially promoted in presence of NO_2. By contrast, nitrates were never detected by NO adsorption on the partially reduced surface. Instead, hyponitrites and reduced *ad*-NO_x species were the dominant species initially formed on defective sites, a period of surface re-oxidation being necessary to the formation of nitrites.

Acknowledgments

The authors wish to thank the French Environmental Agency ADEME for its financial support throughout the Eureka project EU no. 3230 ‘‘Stationocat’’ from which this work was part. We also greatly acknowledge Pr Patrice Bourson (LMOPS, UPV Metz) for his help in Raman analyses and Rhodia-France for supplying ceria–zirconia samples.

References

[1] A. Trovarelli (Ed.), Catalysis by Ceria and Related Materials, Imperial College Press, London, 2002.
[2] P. Vidmar, P. Fornasiero, J. Kašpar, G. Gubitosa, M. Graziani, J. Catal. 171 (1997) 160.
[3] E. Aneggi, M. Boaro, C. de Leitenburg, G. Dolcetti, A. Trovarelli, J. Alloys Compd. 408 (2006) 1096.
[4] J. Kašpar, P. Fornasiero, M. Graziani, Catal. Today 50 (1999) 285.
[5] A.I. Kozlov, D.H. Kim, A. Yezerets, P. Andersen, H.H. Kung Mayfair, M.C. Kung, J. Catal. 209 (2002) 417.
[6] C. Binet, M. Daturi, J.C. Lavalley, Catal. Today 50 (1999) 207.
[7] G. Colon, M. Pijolat, F. Valdivieso, H. Vidal, J. Kaspar, E. Finocchio, M. Daturi, C. Binet, J.C. Lavalley, R.T. Baker, S. Bernal, J. Chem. Soc. Faraday Trans. 94 (1998) 3717.

[8] J.A. Rodriguez, J.C. Hanson, J.Y. Kim, G. Liu, A. Iglesias-Juez, M. Fernandez-Garcia, J. Phys. Chem. B 107 (2003) 3535.
[9] G. Liu, J.A. Rodriguez, J. Hrbek, J. Dvorak, C.H.F. Peden, J. Phys. Chem. B 105 (2001) 7762.
[10] C. Thomas, O. Gorce, C. Fontaine, J.M. Krafft, F. Villain, G. Djéga-Mariadassou, Appl. Catal. B: Environ. 63 (2006) 201.
[11] M. Adamowska, S. Muller, P. Da Costa, A. Krzton, P. Burg, Appl. Catal. B: Environ. 74 (2007) 279.
[12] H.A. Al-Abadleh, V.H. Grassian, Surf. Sci. Rep. 52 (2003) 63.
[13] K.I. Hadjiivanov, G.N. Vayssilov, Adv. Catal. 47 (2002) 307.
[14] S.H. Overbury, D.R. Mullins, D.R. Huntley, L. Kundakovic, J. Catal. 186 (1999) 296.
[15] A. Adamski, E. Tabor, B. Gil, Z. Sojka, Catal. Today 119 (2007) 114.
[16] A. Martinez-Arias, J. Soria, J.C. Conesa, X.L. Seoane, A. Arcoya, R. Cataluna, J. Chem. Soc. Faraday Trans. 91 (1995) 1679.